Journal of Alloys and Compounds 509 (2011) 3617–3622

Contents lists available at ScienceDirect

Journal of Alloys and Compounds

journal homepage: www.elsevier.com/locate/jallcom

Phase transformations behavior in a Cu–8.0Ni–1.8Si alloy

Q. Lei[a], Z. Li[a,b,*], M.P. Wang[a,b], L. Zhang[a], S. Gong[a], Z. Xiao[c], Z.Y. Pan[d]

[a] School of Materials Science and Engineering, Central South University, Changsha, 410083, China
[b] Key Laboratory of Nonferrous Metal Materials Science and Engineering, Ministry of Education, Changsha, 410083, China
[c] Department of Engineering, University of Liverpool, Liverpool, L693 GH, UK
[d] Hunan Nonferrous Metals Holding Group Co., Ltd., Changsha, 410015, China

ARTICLE INFO

Article history:
Received 24 September 2010
Received in revised form
13 December 2010
Accepted 15 December 2010
Available online 23 December 2010

Keywords:
Alloys
Microstructure
Phase transformation
Precipitation
Transmission electron microscopy

ABSTRACT

The phase transformations behavior in a Cu–8.0Ni–1.8Si alloy after different thermal treatments was investigated using transmission electron microscopy. DO_{22} ordering, discontinuous precipitation and continuous precipitation were observed in the alloy. To establish the time-temperature-transformation diagram, samples with different thermal treatments were characterized by transmission electron microscopy. On the basis of SADP analysis, crystal orientations between the copper based matrix and β-Ni_3Si and δ-Ni_2Si precipitates were determined as: $(1\,1\,0)_{Cu}//(1\,1\,0)_{\beta}//(2\,1\,\bar{1})_{\delta}$, $[1\,1\,\bar{2}]_{Cu}//[1\,\bar{1}\,2]_{\beta}//[3\,2\,4]_{\delta}$.

1. Introduction

Copper–matrix alloys are widely used for connector applications because of their high electrical conductivity and high strength [1–3]. The main copper alloy systems whose tensile strength exceeds 1000 MPa are Cu–Ni–Sn [4,5], Cu–Ti [6] and Cu–Be [7]. Cu–Ni–Sn and Cu–Ti alloys have been developed recently as substitutes for the toxic Cu–Be alloys. However, their electrical conductivity is less than 17% IACS (International Annealed Copper Standard), which is much lower than that of Cu–Be alloys (for example, the electrical conductivity of QBe2 has a typical value of 25% IACS). There is a need to develop new alloy with better combination of strength and electrical conductivity. Alloying is an effective method to conduct new Cu-based materials with high strength and good electrical conductivity [8,9]. Cu–Ni–Si-based alloys with high solute concentrations have super high strength and good conductivity, which has a good prospect for substituting for toxic Cu–Be alloys [10]. However, most previous studies on the phase transformation investigated the precipitation process for the Cu–3.1Ni–1.4Si alloys with low solute concentrations [11]. At least four different kinds of precipitation products have been observed by different investigators: DO_{22} ordered structure [10,12], β-Ni_3Si precipitates [13], δ-Ni_2Si precipitates [14–18], and γ-Ni_5Si_2 precipitates [19]. Thus, to say the least, the overall transformation kinetics of Cu–Ni–Si alloys appears to be as complex as other ternary copper alloys [20]. The aging treatment process for the Cu–Ni–Si alloys with high solute concentrations has not been studied systematically up to now. For the Cu–Ni–Si alloys with low solute concentrations, most previous studies on the phase transformations usually investigated the precipitation process at only one temperature or at most a few temperatures. Therefore, a study of the phase transformation behavior for a Cu–Ni–Si-based alloy with high solute concentrations in a wide temperature range has been carried out in this paper.

2. Experimental details

A Cu–8.0Ni–1.8Si (wt%) alloy ingot was prepared using a medium-frequency induction furnace. Pre-specified quantities of Cu and Ni blocks were first melted in the furnace. Cu–Si master alloys of the required quantities were then added into the furnace, producing a chemical composition of the Cu–8.0Ni–1.8Si alloy. The melting and casting operations were carried out in a N_2 atmosphere to prevent the alloy from oxidizing. After surface defects were removed, the ingot was homogenized at 930 °C for 24 h in a N_2+H_2 atmosphere and subsequently rolled at 900 °C in a N_2 atmosphere, reducing the ingot thickness from 20 mm to 4 mm. In our previous research, we have investigated the solution-treatment temperature for Cu–8.0Ni–1.8Si–0.6Sn–0.15Mg alloy systematically and the results indicate that 965 °C is a suitable solution-treatment temperature for high solute concentrations Cu–Ni–Si alloys [10]. Therefore, the resultant strip was solution-treated at 965 °C for 6 h in a N_2+H_2 atmosphere followed by quenching into isothermal bath with

* Corresponding author at: School of Materials Science and Engineering, Central South University, Changsha, 410083, China.
Tel.: +86 731 88830264; fax: +86 731 88876692.
E-mail address: lizhou6931@163.com (Z. Li).

0925-8388/$ – see front matter © 2010 Elsevier B.V. All rights reserved.
doi:10.1016/j.jallcom.2010.12.115

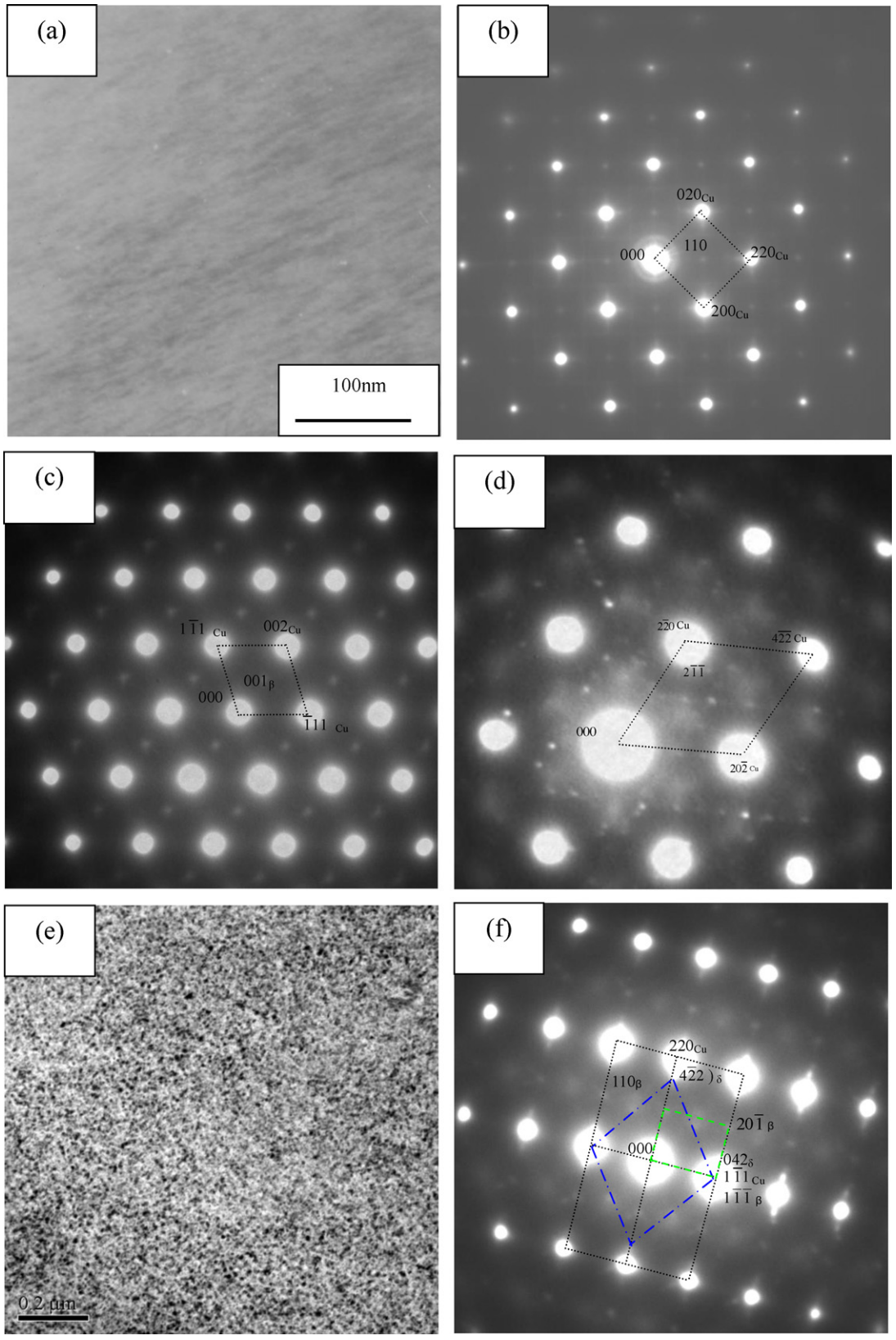

Fig. 1. Samples aged at 450 °C for different times. (a) 15 min, bright field micrograph; (b) 15 min, SADP of $[1\,0\,0]_{Cu}$ zone axis;(c) 15 min, SADP of $[1\,1\,0]_{Cu}$ zone axis; (d) 15 min, SADP of $[1\,1\,1]_{Cu}$ zone axis; (e) 60 min, bright field micrograph; (f) 60 min, SADP of $[1\,1\,\bar{2}]_{Cu}$ zone axis; (g) 60 min, SADP of $[2\,2\,1]_{Cu}$ zone axis; (h) 48 h, bright field micrograph; (i) 48 h, bright field micrograph; (j) 48 h, SADP of $[1\,0\,0]_{Cu}$ zone axis.

different temperatures (450 °C, 550 °C, 650 °C and 750 °C) for various times for isothermal treatment, followed by aging at 450 °C for 8 h, and then water-cooling to room temperature. Specimens for TEM were prepared by argon ion-beam thinning operation with incidence angle of 4°. The microstructures of the foil samples were observed using a Tecnai G^2 20 TEM with an operation voltage of 200 kV.

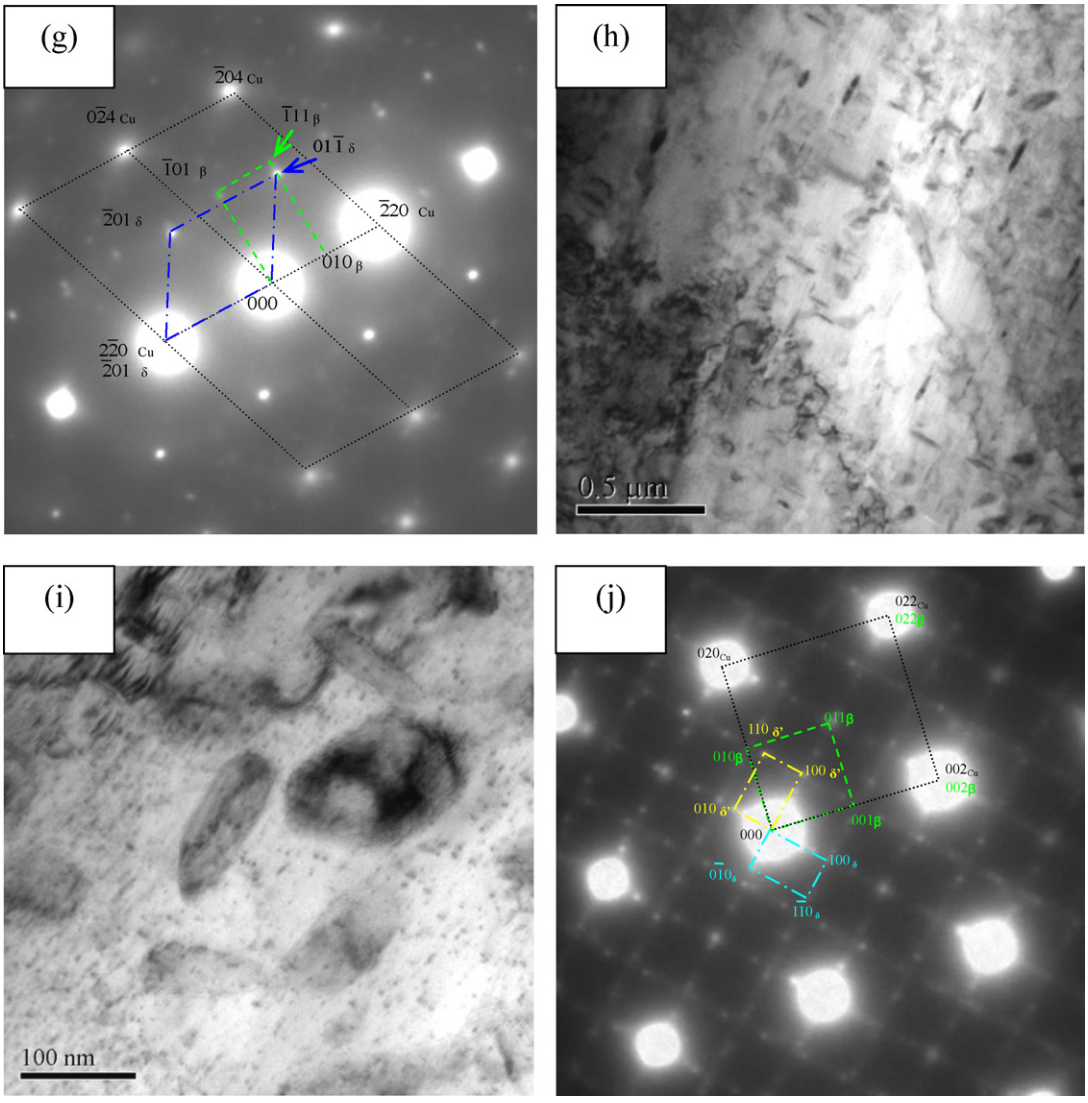

Fig. 1. (*Continued*)

3. Results and discussion

Fig. 1 shows the microstructure evolution of phase transformation of the solution treated samples aged in a salt bath at 450 °C for different times, followed by water-cooling. When the samples were kept at 450 °C for 15 min, a few precipitates can be seen in Fig. 1a. The corresponding select area diffraction patterns (SADP) are presented in Fig. 1b, c and d. The super-lattice diffraction spots between $(0\,0\,0)_{Cu}$ and $(2\,2\,0)_{Cu}$ appeared clearly in Fig. 1b, between $(0\,0\,0)_{Cu}$ and $(0\,0\,2)_{Cu}$ in Fig. 1c and between $(0\,0\,0)_{Cu}$ and $(4\,\bar{2}\,\bar{2})_{Cu}$ in Fig. 1d (at the position of $(2\,\bar{1}\,\bar{1})_{Cu}$), which means that the ordering occurred at early stage of the aging process. From Fig. 1d, it can be distinguished that the type of the ordering is DO_{22} ordering because the typical $(2\,\bar{1}\,\bar{1})_{Cu}$ reflection is unique to DO_{22} ordering [12]. However, the $L1_2$ ordering cannot be clarified in this test alloy because all the $L1_2$ super-lattice reflection overlaps with some of the DO_{22} super lattice reflections.

When increase the keeping aging time to 60 min, precipitates can be found in bright-field micrograph, as shown in Fig. 1e. The corresponding SADPs are shown in Fig. 1f and g. The electron beam axis of the SADP of Fig. 1f is parallel to $[1\,1\,\bar{2}]_{Cu}$; and that of Fig. 1g is parallel to $[2\,2\,1]_{Cu}$. There were two kinds of precipitates, which can be indentified as δ-Ni_2Si and β-Ni_3Si. The δ-Ni_2Si structure was found by Toman [20] to have structural parameters of $a = 0.703$ nm, $b = 0.499$ nm and $c = 0.372$ nm. The β-Ni_3Si structure was a simple cubic lattice with $a = 3.51$ nm [21–23]. From the analysis in Fig. 1f, the crystal orientations between the cupper based matrix and β-Ni_3Si and δ-Ni_2Si precipitates were determined as: $(1\,1\,0)_{Cu}//(1\,1\,0)_\beta//(2\,1\,\bar{1})_\delta$, $[1\,1\,\bar{2}]_{Cu}//[1\,\bar{1}\,2]_\beta//[3\,2\,4]_\delta$.

When increase the keeping aging time further to 48 h, i.e. the samples undergoing overaging treatment, the precipitates in the bright-field micrograph (Fig. 1h) grew bigger than those in Fig. 1e. Two variants of precipitates grew vertically (Fig. 1i). According to the analysis of SADP in Fig. 1j, the two kinds of precipitates can be expressed as δ-Ni_2Si and δ′-Ni_2Si precipitates, which have the same crystal structure. Between the bigger precipitates, there were a mass of nano-scale particles (Fig. 1i). From the SADP in Fig. 1j, four kinds of diffraction spots can be distinguished. They came from the electron diffractions of Cu-matrix, β-Ni_3Si and δ-Ni_2Si and δ′-Ni_2Si precipitates, respectively. The orientation relationship between the precipitates and Cu-matrix, according to the analysis of Fig. 1j, which can be expressed as that: $(0\,2\,2)_{Cu}//(0\,2\,2)_\beta$ $(1\,0\,0)_\delta$, $(0\,\bar{2}\,2)_{Cu}$ $(0\,\bar{2}\,2)_\beta//(1\,0\,0)_{\delta'}$; $[1\,0\,0]_{Cu}//[1\,0\,0]_\beta//[0\,0\,1]_{\delta'}//[0\,0\,1]_\delta$.

The structure of specimens isothermal treated at 550 °C for 10 s and 30 s, immediately followed by aging at 450 °C for 8 h

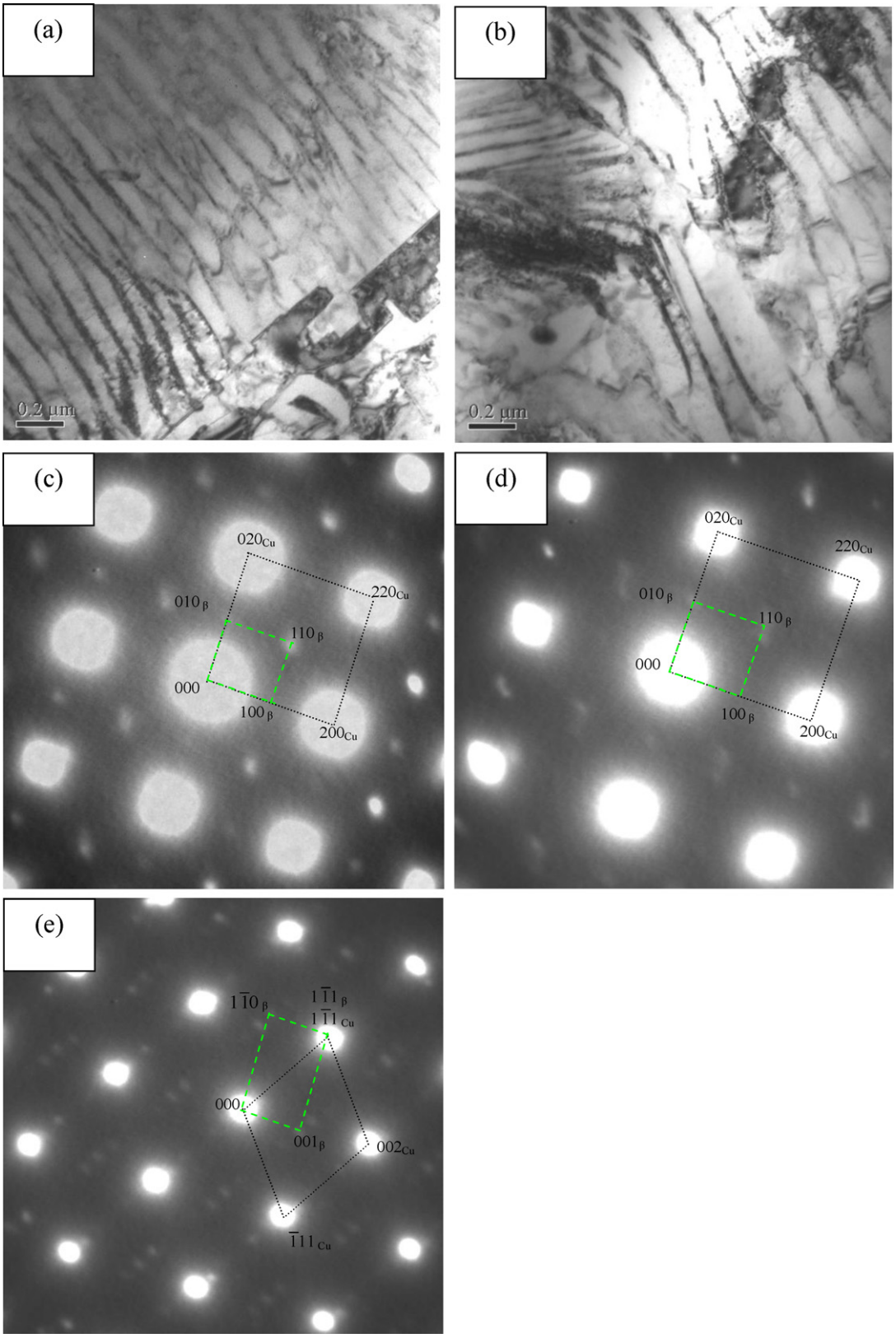

Fig. 2. Sample aged at 550 °C for different times. (a) 10 s, bright field micrograph; (b) 30 s, bright field micrograph; (c) 10 s, SADP of $[0\,0\,1]_{Cu}$ zone axis; (d) 30 s, SADP of $[0\,0\,1]_{Cu}$ zone axis; (e) 10 s, SADP of $[1\,1\,0]_{Cu}$ zone axis.

are shown in Fig. 2. A well-developed discontinuous precipitation structure can be seen in Fig. 2. The whole specimen had a cellular structure, which indicates that the discontinuous precipitation reaction was already complete in this specimen. The discontinuous precipitation microstructure in the alloy can be seen clearly in Fig. 2a and b. The corresponding SADPs from the matrix area in this

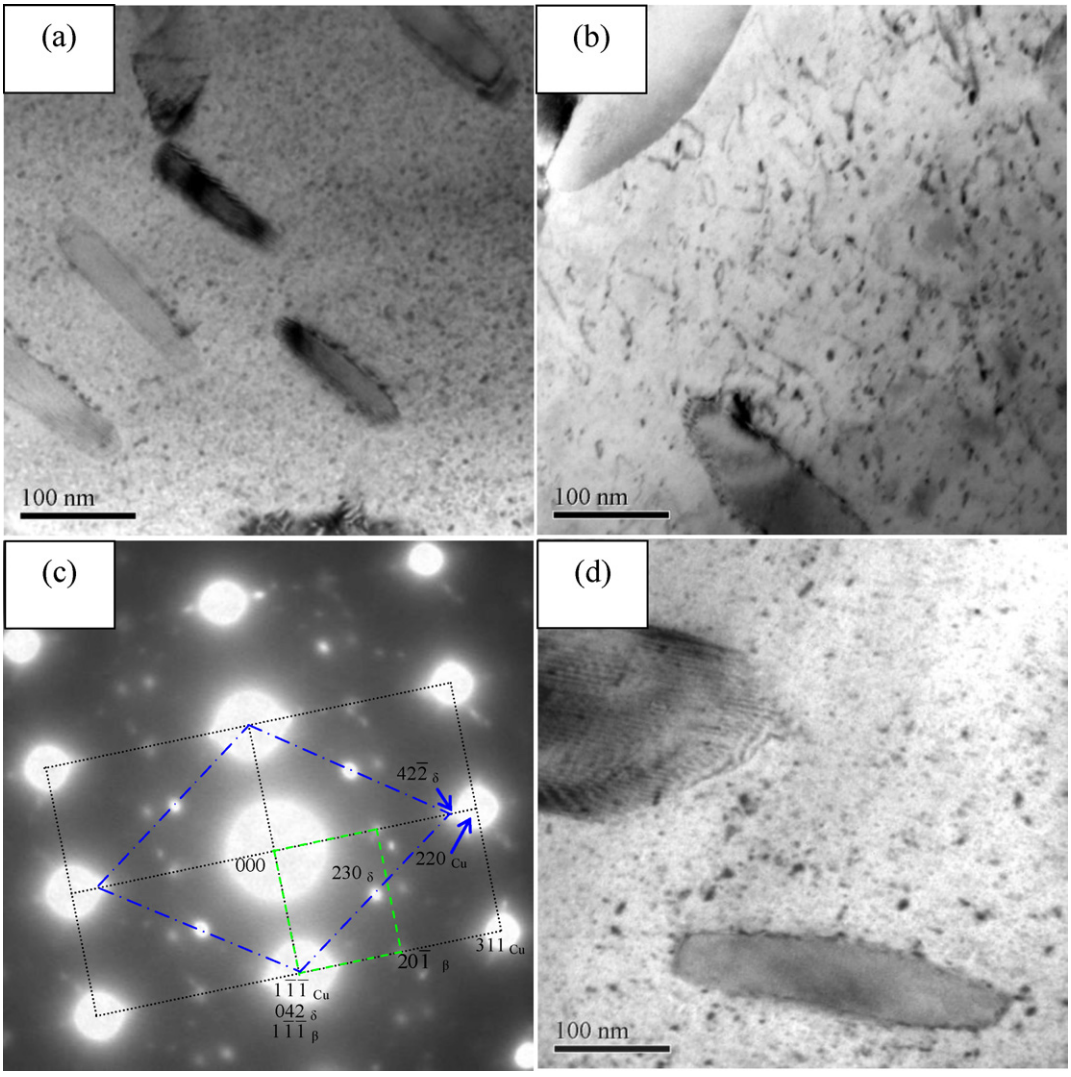

Fig. 3. Bright field micrograph and select area diffraction pattern of Cu–8.0Ni–1.8Si alloy quenched to 650 °C and 750 °C and isothermally treated for different times. (a) 650 °C for 30 s, bright-field micrograph; (b) 650 °C for 300 s, bright field micrograph; (c) SADP of (a), whose beam direction is along $[1\,1\,\bar{2}]_{Cu}$; (d) 750 °C for 30 s, bright field micrograph.

specimen are shown in Fig. 2c, d and e, respectively. According to the SADPs (Fig. 2c, d and e), the discontinuous precipitates were β-Ni_3Si phase particles. From Fig. 2d and e, slight split-up of the diffraction spots of $(1\,1\,0)_{\beta}$ and $(0\,0\,1)_{\beta}$ occurred. The discontinuous precipitation formed the lamellar structure. The lamellar cellular structure grew bigger with increasing the isothermal time (Fig. 2a and b). The discontinuous precipitation in the Cu–Ni–Si alloy with high solute concentration was observed for the first time.

Fig. 3a shows the micrograph of Cu–8.0Ni–1.8Si alloy quenched into 650 °C for 30 s and 300 s, immediately followed by aging at 450 °C for 8 h. There were two kinds of precipitates in the bright field micrograph (Fig. 3a). The bigger ones appeared with dimensions of 100 nm (in length) × 30 nm (in thickness). The smaller ones in Fig. 3a were only 5–6 nm in size. Fig. 3b presents the micrograph of Cu–8.0 Ni–1.8 Si alloy quenched into 650 °C for 300 s. Two kinds of precipitates grew bigger than those in Fig. 3a. The bigger precipitates grew to dimensions of 300 nm (in length) × 90 nm (in thickness). The smaller precipitates also grew bigger and their dimensions are between 8 and 10 nm. Fig. 3c shows SADP of Fig. 3a. According to Fig. 3c, the two kinds of precipitates were determined to be β-Ni_3Si phase [11,23] and δ-Ni_2Si phase [24,25].

Fig. 3d presents the micrograph of Cu–8.0 Ni–1.8 Si alloy quenching into 750 °C for 30 s, followed by aging at 450 °C for 8 h. The bigger β-Ni_3Si precipitates have a dimensions of 400 nm (in length) × 50 nm (in thickness), and the size of small δ-Ni_2Si precipitates is about 7–8 nm (Fig. 3d), which is bigger than that in Fig. 3a.

The results for the phase transformation research can be summarized by the time–temperature–transformation diagram as shown in Fig. 4. Three curves were constructed for DO_{22} ordering, discontinuous precipitation (cellular structure) and continuous precipitation (δ-Ni_2Si), respectively. When the supersaturated solid solution (SSS) of Cu–8.0Ni–1.8Si alloy was aged at low temperature of 450 °C, the phase transformations were rich and interesting. It is clearly seen that DO_{22} ordering took place at the early stage of the decomposition process as a separate precipitation, and then continuous precipitation occurred [26]. When the alloy was isothermal treated at 550 °C for a short time, discontinuous precipitation occurred along the grain boundary in the alloy. When the aging temperature reached higher than 600 °C, continuous precipitation appeared in the alloy directly without ordering. It is clear that the higher aging temperature, the earlier decomposition occurs. These experimental

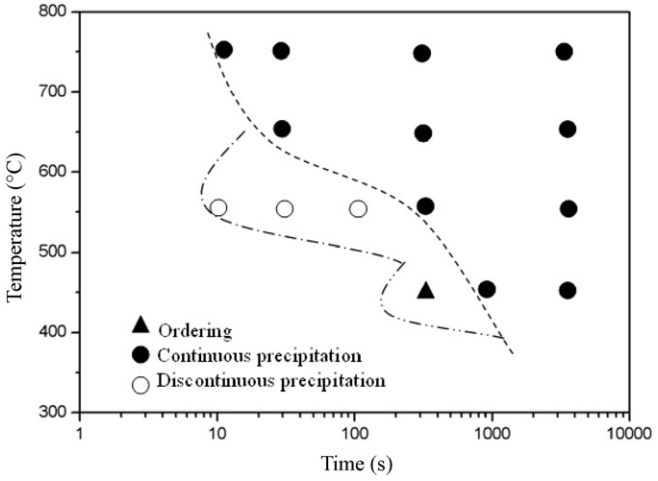

Fig. 4. TTT diagram for the Cu–8.0Ni–1.8Si alloy obtained by TEM characterization. Symbols of "▲, ● and ○" in the TTT diagram represent the ordering, continuous precipitation (δ-Ni_2Si) and discontinuous precipitation (cellular structure), respectively.

results were similar to the research results presented by Zhao [27].

4. Conclusions

The phase transformations behavior of Cu–8.0Ni–1.8Si alloy during aging at different heat treat conditions after solution treatment has been studied. The main conclusion remarks can be summarized as follows:

After solution treatment, followed by different conditions of isothermal treatment and aging process, DO_{22} ordering, discontinuous precipitation (cellular structure) and continuous precipitation (δ-Ni_2Si) occurred in the alloy.

Two kinds of precipitates of β-Ni_3Si and δ-Ni_2Si were determined by the TEM characterization in the alloy. Crystal orientations between the cupper based matrix and the β-Ni_3Si and δ-Ni_2Si precipitates were determined as: $(1\,1\,0)_{Cu}//(1\,1\,0)_{\beta}//(2\,1\,\bar{1})_{\delta}$, $[1\,1\,\bar{2}]_{Cu}//[1\,\bar{1}\,2]_{\beta}//[3\,2\,4]_{\delta}$.

When the samples were overaging treated at 450 °C for 48 h, four kinds of phases (Cu-matrix, β-Ni_3Si, δ-Ni_2Si and δ′-Ni_2Si) were distinguished in the samples and the orientation relationship between Cu-matrix and precipitates can be expressed as: $(0\,2\,2)_{Cu}//(0\,2\,2)_{\beta}//(1\,0\,0)_{\delta}$, $(0\,\bar{2}\,2)_{Cu}//(0\,\bar{2}\,2)_{\beta}(1\,0\,0)_{\delta'}$, $[1\,0\,0]_{Cu}[1\,0\,0]_{\beta}[0\,0\,1]_{\delta'}//[0\,0\,1]_{\delta}$.

A detailed TTT diagram for the isothermal decomposition of the Cu–8.0Ni–1.8Si alloy was established based on extensive TEM characterizations.

Acknowledgments

The authors are pleased to acknowledge the financial support of this research by the Nonferrous Metals Science Foundation of HNG-CSU. They are also grateful to Z. Zhang and B. Tang for the TEM operations.

References

[1] Z.Q. Wang, Y.B. Zhong, G.H. Cao, et al., J. Alloys Compd. 479 (2009) 303–306.
[2] W.A. Badawy, K.M. Ismail, A.M. Fathi, J. Alloys Compd. 484 (2009) 365–370.
[3] B.D. Long, H. Zuhailawati, M. Umemoto, Y. Todaka, R. Othman, J. Alloys Compd. 503 (2010) 228–232.
[4] W.S. Jeon, C.C. Shur, J.G. Kim, S.Z. Han, Y.S. Kim, J. Alloys Compd. 455 (2008) 358–363.
[5] M. Masamichi, O. Yoshikiyo, Mater. Trans. JIM 29 (1994) 903–910.
[6] W.A. Soffa, D.E. Laughlin, Mater. Sci. 49 (2004) 347–366.
[7] H. Tsubakino, R. Nozato, A. Yamamoto, Mater. Sci. Technol. 19 (1993) 288–294.
[8] J. Wang, S. Jin, C. Leinenbach, A. Jacot, J. Alloys Compd. 504 (2010) 159–165.
[9] Q. Lei, Z. Li, Z.Y. Pan, M.P. Wang, Z. Xiao, C. Chen, Trans. Nonferrous Met. Soc. China 20 (2010) 1006–1011.
[10] Z. Li, Z.Y. Pan, Y.Y. Zhao, Z. Xiao, M.P. Wang, J. Mater. Res. 24 (2009) 2123–2129.
[11] S. Suzuki, N. Shibutani, K. Mimura, M. Isshiki, Y. Waseda, J. Alloys Compd. 417 (2006) 116–120.
[12] D.M. Zhao, Q.M. Dong, P. Liu, B.X. Kang, J.L. Huang, Z.H. Jin, Mater. Chem. Phys. 79 (2003) 81–86.
[13] H. Xie, L. Jia, Z.L. Lu, Mater. Charact. 60 (2009) 114–118.
[14] M.G. Corson, Electrical World 89 (1927) 137–139.
[15] Z.Y. Pan, M.P. Wang, Z. Li, C.P. Deng, S.H. Li, Y.L. Jia, Heat Treat. Met. 7 (2007) 55–59.
[16] S.A. Lockyer, F.W. Noble, J. Mater. Sci. 29 (1994) 218–226.
[17] R.J. Grylls, C.D.S. Tuck, Scripta Mater. 43 (1996) 121–126.
[18] M. Okamoto, Trans. Inst. Met. Jnn. 3 (1939) 336.
[19] W.D. Robertson, E.G. Grenier, V.F. Nole, Trans. Met. Soc. AIME 221 (1961) 503.
[20] K. Toman, Acta Crystallogr. 5 (1952).
[21] N.F. Lashko Dokl, Akad. Nauk. SSSR 81 (1951) 606.
[22] Q. Lei, Z. Li, M.P. Wang, L. Zhang, Y.L. Jia, Mater. Sci. Eng. A 527 (2010) 6728–6733.
[23] A.T. Dutra, P.L. Ferrandini, R. Caram, J. Alloys Compd. 432 (2007) 167–171.
[24] R. Monzen, C. Watanabe, Mater. Sci. Eng. A 483 (2008) 117–119.
[25] R. Monzen, C. Watanabe, Z.G. Zhang, J. Soc. Mater. Sci. Jpn. 54 (2005) 717–723.
[26] Z. Sun, C. Laitem, A. Vincent, Mater. Sci. Eng. A 477 (2008) 145–152.
[27] J.C. Zhao, M.R. Notis, Acta Mater. 46 (1998) 4203–4218.